Simulation of flow in a pulsed-jet mixer using a volume of fluid model

D. Eldin[1], S. Parks[1], C. Petty[1] & A. Bénard[2]
[1]*Department of Chemical Engineering and Materials Science*
[2]*Department of Mechanical Engineering,*
Michigan State University

Abstract

Pulsed-jet mixers (PJM) are often used to suspend a solid phase in a liquid phase within very large tanks. In this study, a commercial CFD code (Fluent 6.0) is used to simulate the axisymmetric flow field induced by a PJM symmetrically situated in a cylindrical tank. The simulation uses a volume-of-fluid model for an air/water system with a standard k-ε model for the Reynolds stress. A large-scale periodic recirculation zone is established within the tank and provides a means to suspend solid particles. Particle trajectory calculations are used to identify potential regions of high wear on the bottom of the tank and within the jet nozzle. The simulation supports the conclusion that a PJM should be able to suspend 100-micron diameter particles with a density three times larger than water. However, under the same operating conditions, 500-micron diameter particles with densities equal to or larger than 3000 kg/m^3 will settle to the bottom of the tank.
Keywords: volume-of-fluid model, discrete phase model, solid/liquid suspension, mixing, pulsed-jet mixer.

1 Introduction

Large amounts of radioactive waste are presently stored in very large underground tanks at DOE's Hanford Site in the State of Washington. Plans are developing to vitrify the waste to produce a stable glassy state for long term disposal in remote locations. Before the waste can be sent to the vitrification pre-treatment plant, the liquid and sludge in the underground storage tank must be mixed to form a slurry that can be mobilized (pumped). As noted by Daymo [1],

Advances in Fluid Mechanics V, A. Mendes, M. Rahman & C. A. Brebbia (Editors)

multiple pulsed-jet mixers (PJMs) are a cost-effective technology for suspending concentrated radioactive sludge material in very large tanks and are presently being evaluated for this application.

The main advantage of PJM technology over other mixers is that they have no moving parts inside the tank. The PJM has a frustoconical effluent nozzle (see Figure 1). A vacuum is created within the cylindrical chamber of the PJM to draw a relatively small amount of the suspension into the cylindrical chamber. Once full, the pressure difference between the two control surfaces shown in Figure 1 is reversed and the fluid is discharged at a high velocity near the bottom of the tank. The repetitive suction/discharge action of the mixer mobilizes the radioactive sludge near the bottom of the tank by creating large-scale toroidal recirculation flows.

Patwardham [2] recently studied the performance of conventional jet mixing under statistically stationary conditions using CFD. CFD is used hereinafter to develop a preliminary evaluation of the mixing performance of a pulsed-jet mixer for a temporally periodic (and spatially inhomogeneous) flow field. FLUENT 6.0, which employs a finite volume method to discritize the governing transport equations, was used to support the simulation. Particle trajectory calculations are used to quantify the motion of discrete particles in the flow. This paper stems from a recently completed Master of Science thesis by D. Eldin [3].

2 Methodology and scope of the simulation

The waste tanks in the field are very large and may need several PJMs to resuspend the radioactive sludge. In this simulation, a single PJM was symmetrically situated in a flat bottom tank with no internal piping (see Figure 1). The flow field is axisymmetric and unsteady. The suction phase of the PJM is three times as long as the drive phase. The tank and the pulsed-jet mixer are open at the top. The control surface within the jet is at the same height as the control surface of the tank. Under quiescent conditions (i.e., no flow), the liquid phase occupies 95% of the jet volume. At the end of the drive phase, the liquid phase occupies 8% of the jet volume, which is about the volume of the nozzle.

The inner diameter and the height of the tank are, respectively, 0.91 m and 1.29 m. The cylindrical part of the mixer has a height of 1.07 m and an inner diameter of 0.25 m. A conical nozzle, which has a contraction ratio of 2.5:1, is attached to the bottom of the cylinder. The end of the nozzle is 0.048 m above the bottom of the tank. The length of the pulsed-jet mixer is 1.24 m.

A volume-of-fluid model supported by a standard k-ε closure model for the Reynolds stress was used to track the air-liquid interface and to simulate the flow field within the PJM and tank. The top of the tank is modeled as a free surface. The velocity at the control surface S_1 (see Figure 1) is calculated based on the required time for the drive phase (2 seconds) and the suction phase (6 seconds). A constant pressure of 0 Pa is set at control surface S_2. A discrete particle model was used to determine the motion of solid spherical particles suspended in water. The following physical properties were used in the simulation: liquid phase

Advances in Fluid Mechanics V, A. Mendes, M. Rahman & C. A. Brebbia (Editors)

density, 998 kg/m^3; liquid phase viscosity, 0.001003 kg/(m-s); air phase density, 1.225 kg/m^3; air phase viscosity, 0.000017894 kg/(m-s); and, solid phase density, 3000 kg/m^3.

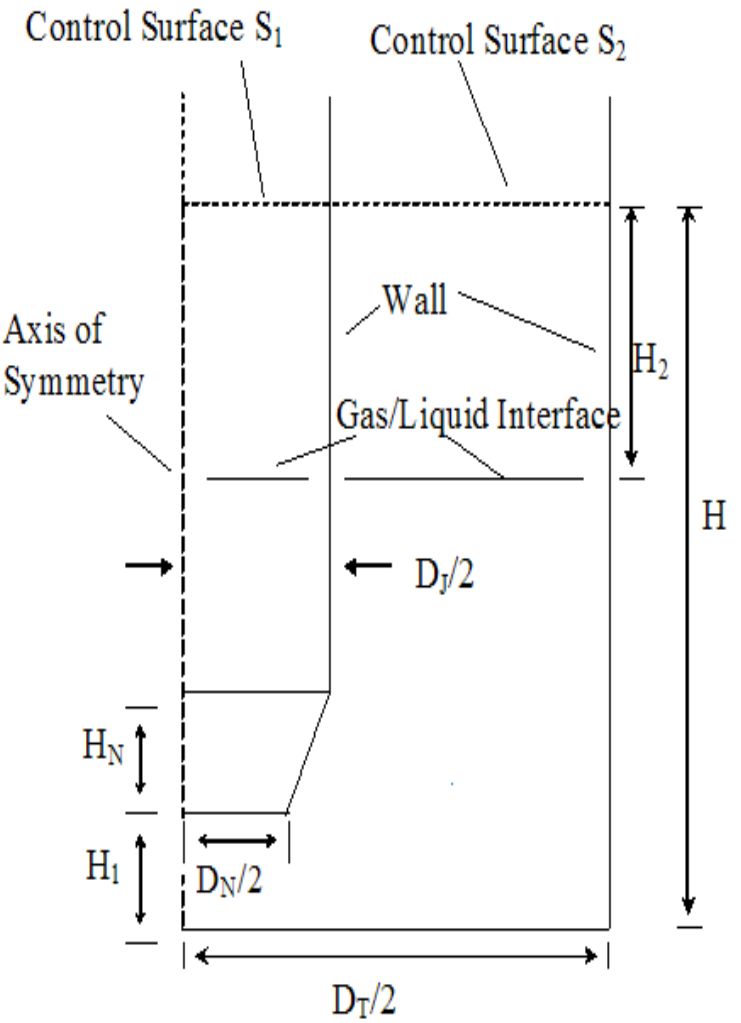

Figure 1: Geometry of pulsed-jet mixer and tank (D_J/D_T = 0.28, H/D_T = 1.41, H_1/D_N = 0.46, D_N/D_J = 0.40, H_N/D_J = 0.69, H_2/D_T variable, D_T = 0.91 m).

Advances in Fluid Mechanics V, A. Mendes, M. Rahman & C. A. Brebbia (Editors)

The simulation assumes that the unsteady flow field is axisymmetric with a plane of symmetry containing the axis of the tank. Therefore, only half of the geometry was meshed by GAMBIT 2.0 (see Fluent User Manual [4]). A non-uniform grid was used inasmuch as a finer grid is needed near the fluid/solid interfaces due to the no slip boundary condition. Also, an unstructured grid was used for the nozzle portion of the geometry and the triangular part of the flow domain adjacent to the nozzle.

The number of computational cells used in the simulation was 13,894. The grid was fine enough to allow for a grid independent solution, but course enough to yield a converged result in a reasonable amount of time. A continuity residual of 0.00014 kg/s was used as a condition for convergence. FLUENT default values were used for the components of the velocity, the turbulent kinetic energy, and the turbulent dissipation. Two hundred time steps were needed to simulate the 2s-drive phase and six hundred time steps were needed for the 6s-suction phase. It took approximately one hour to simulate the drive phase and 3 hours to simulate the suction phase.

No-slip boundary conditions were imposed on all solid/fluid interfaces (i.e., tank walls, tank bottom, and PJM walls). A velocity inlet boundary was specified at a control surface located at the top of the jet-mixer and, as indicated above, a pressure outlet boundary was specified at the control surface at the top of the tank. The mean velocity on the "inlet boundary" during the drive phase was 0.4803 m/s. The mean velocity on the "inlet boundary" during the suction phase was – 0.1601 m/s. The flow field was initialized from the values at the inlet. The simulation was allowed to develop to a periodic state before discrete particles were introduced into the flow field. Monitors in the computation domain were employed to track the velocity as a function of time at different locations.

The particle diameters encountered in practice may range from submicron to more than 600 microns. Particle trajectories were developed for 100-micron diameter particles and for 500-micron diameter particles. The particles were introduced into the flow field with an initial velocity of zero. The boundary condition on the discrete particles included reflection at a solid/fluid boundary and escape at a fluid/fluid boundary (see Fluent User's Manual [4]).

3 Mathematical model

A volume-of-fluid (VOF) model, as described by Hirt and Nichols [5] and in the Fluent User's Manual [4], was used to simulate the flow field. Air is chosen as the primary phase and water as the secondary phase. The divergence of the mixture velocity is zero: $\nabla \cdot < \underline{u} > = 0$. The VOF model also assumes that no mass transfer occurs between the two immiscible phases (i.e., air and water). Therefore, the tracking of the air/water interface (see Figure 1) is accomplished by solving the continuity equation for the volume fraction of the secondary phase (i.e., water):

$$\frac{\partial < \alpha_2 >}{\partial t} + < \underline{u} > \cdot \nabla < \alpha_2 > = 0 \ . \qquad (1)$$

Advances in Fluid Mechanics V, A. Mendes, M. Rahman & C. A. Brebbia (Editors)

The volume fraction α_1 of the primary phase (air) is determined from the condition, $<\alpha_1>+<\alpha_2>=1$. The mixture momentum per unit volume in the VOF model is governed by

$$\frac{\partial}{\partial t}(<\rho><\underline{u}>)+\nabla\cdot(<\rho><\underline{u}><\underline{u}>)=-\nabla<P>+<\rho>\underline{g} + \nabla\cdot(2<\mu><\underline{\underline{S}}>-<\rho><\underline{u}'\underline{u}'>) \quad , \tag{2}$$

where $<\underline{\underline{S}}>$ is the mean strain rate and the last term in the above equation is the Reynolds stress. The mean density of the mixture is given by $<\rho>\equiv<\alpha_1>\rho_1+<\alpha_2>\rho_2$, where ρ_1 is the density of air and ρ_2 is the density of water. Also, the mean viscosity of the mixture is $<\mu>\equiv<\alpha_1>\mu_1+<\alpha_2>\mu_2$, where μ_1 is the viscosity of air and μ_2 is the viscosity of water.

The VOF model supported by Fluent 6.0 uses a Boussinesq closure for the Reynolds stress:

$$-\rho<\underline{u}'\underline{u}'>=2\mu_e<\underline{\underline{S}}>-\frac{2}{3}<\rho>k\,\underline{\underline{I}} \quad . \tag{3}$$

The scalar-valued eddy viscosity is related to the kinetic energy and dissipation of the local turbulence as well as the mean density of the mixture: $\mu_e = C_\mu <\rho> k^2/\varepsilon$. Transport equations for k and ε are used to determine the local kinetic energy and dissipation of the turbulence:

$$\frac{\partial(<\rho>k)}{\partial t}+\nabla\cdot(<\rho>k<\underline{u}>) = \nabla\cdot[(<\mu>+\frac{\mu_e}{\sigma_k})\nabla k] - <\rho><\underline{u}'\underline{u}'>:\nabla<\underline{u}>-<\rho>\varepsilon \tag{4}$$

$$\frac{\partial(<\rho>\varepsilon)}{\partial t}+\nabla\cdot(<\rho>\varepsilon<\underline{u}>)=\nabla\cdot[(<\mu>+\frac{\mu_e}{\sigma_\varepsilon})\nabla\varepsilon] - C_{1\varepsilon}<\rho><\underline{u}'\underline{u}'>:\nabla<\underline{u}>\frac{\varepsilon}{k}-C_{2\varepsilon}<\rho>\frac{\varepsilon^2}{k} \quad . \tag{5}$$

The simulation uses a standard wall function near fluid/solid interfaces (see the Fluent User's Manual [4] for details). The following closure parameters complete the definition of the k-ε model for the Reynolds stress:

$$\sigma_k=1.0\,;\ \sigma_\varepsilon=1.3\,;\ C_{1\varepsilon}=1.44\,;\ C_{2\varepsilon}=1.92;\ \text{and}\ C_\mu=0.09\,.$$

A discrete phase model is used to determine the trajectories of individual solid particles in the flow field. The direct influence of turbulent fluctuations on the trajectories is neglected. The mean position and the mean velocity of a particle are governed by the following equations:

Advances in Fluid Mechanics V, A. Mendes, M. Rahman & C. A. Brebbia (Editors)

$$\frac{d < \underline{x}_P >}{d t} = < \underline{u}_P > \tag{6}$$

$$\frac{d < \underline{u}_P >}{d t} = F_D + \frac{\rho_P - < \rho >}{\rho_P} \underline{g} \quad . \tag{7}$$

F_D is the drag per unit particle mass and depends on the slip velocity and the Reynolds number:

$$F_D = \frac{18 < \mu > C_D \, Re}{\rho_P d_p^2 24} (< \underline{u} > - < \underline{u}_p >) . \tag{8}$$

In the above equation, $< \underline{u} >$ is the mean velocity of the air/water mixture and $< \underline{u}_p >$ is the mean velocity of the solid particle. The mean density and the mean viscosity of the fluid mixture are defined above. ρ_P is the density of an individual particle of diameter d_P. The particle Reynolds number is defined as follows

$$Re \equiv \frac{< \rho > d_P \left| < \underline{u} > - \underline{u}_p \right|}{< \mu >} . \tag{9}$$

The simulation uses the following empirical equation for the drag coefficient (see Fluent User's Manual [4]):

$$C_D = \frac{24}{Re} (1 + 0.186 \, Re^{0.653}) + \frac{0.437 \, Re}{717 + Re} . \tag{10}$$

4 Results

Figure 2 shows the instantaneous velocity magnitude and vectors at the middle of the drive phase of Cycle 3. The air/water interface has moved halfway down the jet and slightly higher in the annular region. Although the overall size of the toroidal recirculation zone remains the same during the drive phase, the center is closer to the corner of the tank at the midpoint of the drive. Due to the high velocity coming form the nozzle, the bottom of the tank and the bottom quarter of the wall of the tank has a higher velocity than at the beginning of the drive phase. The velocity in the cylindrical part of the jet is nearly uniform and the high velocity at the nozzle now extends over the entire exit area of the nozzle.

Figure 3 shows the instantaneous velocity magnitude and vectors at the middle of the suction phase of Cycle 3. The interface has moved back to the same location as the middle of the drive phase. The overall size of the recirculation zone is larger than during the drive phase with approximately two-thirds of the flow field participating in the recirculation region. The center of the recirculation zone has moved slightly upward and away from the wall of the tank. The vectors in the top third of the annular region are pointed in the downward direction. The high velocities at the bottom of the tank and near the

Advances in Fluid Mechanics V, A. Mendes, M. Rahman & C. A. Brebbia (Editors)

wall during the drive phase have diminished. The velocity field in the nozzle of the PJM contains a small-scale recirculation zone. This recirculation pattern does not develop during the drive phase. The recirculation flow formed in the nozzle during the suction phase moves toward the axis of symmetry within 0.0001 s of the drive phase and has vanished altogether after 1 s (see Figure 2).

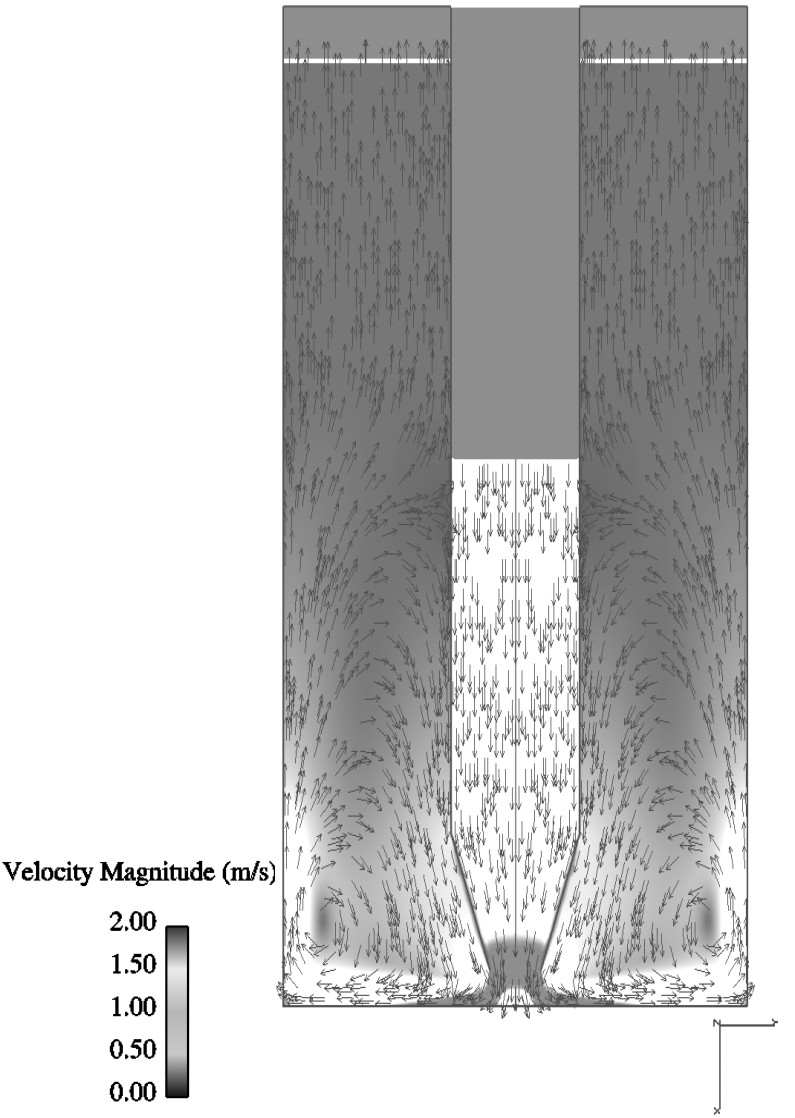

Figure 2: Instantaneous contours of velocity magnitude and velocity vectors at the middle of the drive phase (max velocity = 3.50 m/s).

Advances in Fluid Mechanics V, A. Mendes, M. Rahman & C. A. Brebbia (Editors)

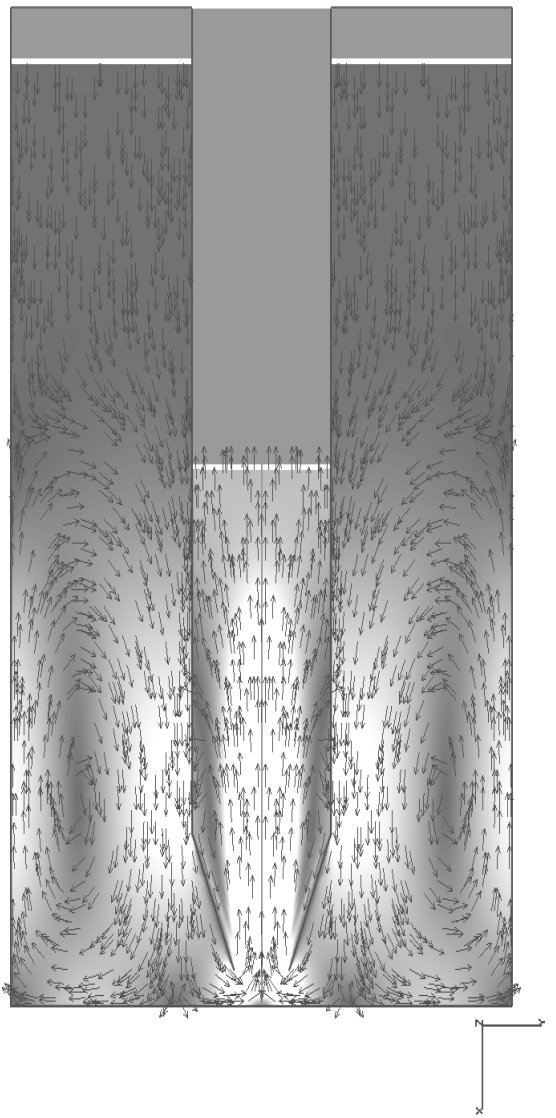

Figure 3: Instantaneous contours of velocity magnitude and velocity vectors at the middle of the suction phase (max velocity = 1.70 m/s; gray scales are qualitatively similar to those shown in Figure 2).

Two significant stagnation points develop during the PJM cycle: one during the drive phase and another during the suction phase. As expected, a stagnation point occurs at the bottom of the tank on the axis of symmetry just below the jet nozzle during the drive phase. It can be seen that the vectors in this region point

Advances in Fluid Mechanics V, A. Mendes, M. Rahman & C. A. Brebbia (Editors)

towards the bottom of the tank and are unable to turn. During the suction phase the stagnation point has shifted. It occurs where the streamlines split the circulating region and flow returning to the nozzle of the jet.

The gauge pressure on the control surface S_2 is specified as 0 Pa during the drive phase, which implies that the absolute pressure on S_2 is one atmosphere or 101,325 Pa. Half way through the drive phase the pressure difference between control surface S_1 (see Figure 1) and control surface S_2 is about 14, 435 Pa. Towards the end of the drive phase, the pressure difference increases to about 19,397 Pa.

Forty solid particles were introduced into the flow field at the beginning of Cycle 3 and tracked for the entire cycle (drive phase and suction phase). Ten particles were placed at four different elevations in the tank, seven in the annular region and three in the jet region. Particles were placed between the nozzle and the bottom of the tank, in the recirculation zone, directly above the recirculation zone and in the area where the bulk of the fluid does not enter the circulating region. Placing the particles at different starting position provided insights on the influence of the starting position on particle impingement and particle separation (see Eldin [3]).

Two critical zones were found where particles might tend to drop from the recirculating region. In the drive phase, this is near the axis of symmetry when exiting the nozzle. In the suction phase, there is a limiting streamline between the recirculation zone and the fluid that is pulled back into the jet. If the particles follow this limiting streamline they may hit the bottom of the tank. Particles with diameters less than 100 μm on the bottom of the tank can be resuspended by the action of the recirculation zone. On the other hand, the recirculation flow cannot resuspend particles larger than 500 μm in diameter unless the jet velocity is increased significantly. After a few cycles, all large particles end up at the bottom of the tank near the outer wall under the operating conditions studied.

5 Conclusions

The VOF model is an effective tool for tracking the air/water interface of a pulsed-jet mixer and for tracking solid particles within the tank. The periodic flow develops rapidly after a few PJM cycles. It is most significant that a secondary flow develops within the nozzle during the suction phase of the cycle. This is an important observation inasmuch as the repetitive abrasive action of the suspension may cause a serious wear problem on the internal surface of the PJM. Similarly, surfaces on the outer wall and on the bottom of the tank may also be susceptible to wear due to the cyclical abrasive grinding motion of the suspension. Furthermore, the high velocity at the nozzle exit during the drive phase may also cause wear on the tank bottom due to particle impingement.

The size of the large-scale toroidal recirculation zone increases during the suction phase compared to the drive phase. Under the conditions of the simulation, particles with diameters less than 100μm do not significantly migrate across recirculation streamlines during the suction or drive phases; however, 500-μm diameter particles do cross these streamlines by centrifugal action and

Advances in Fluid Mechanics V, A. Mendes, M. Rahman & C. A. Brebbia (Editors)

gravity. Thus, a dilute dispersed phase having a particle size distribution with a maximum particle size less than 100 μm will remain suspended over a full cycle of the PJM. A PJM operating at a higher velocity is needed to keep 500-μm diameter particles suspended.

Acknowledgments

The authors thank Dr. Brigette Rosendall of Bechtel for suggesting this simulation as a case study example for a combined research and curriculum development project on computational multiphase transport phenomena funded by the National Science Foundation (NSF/EEC 9980325). This research was also partially supported by a National Science Foundation GOALI grant (NSF/CTS 0083227). The authors thank the National Science Foundation for their support of this research.

References

[1] Daymo, E. A., Industrial Mixing Techniques for Hanford Double-Shell Tanks, Pacific Northwest National Laboratory, PNNL-11725, UC-721, 1997.
[2] Patwardhan, A.W., *CFD Modeling of Jet Mixed Tanks*, Pergamon Press, 2001.
[3] Edin, D. *Computational Fluid Dynamics Simulation of a Pulsed-Jet Mixer*, Master of Science Thesis, Department of Chemical Engineering and Materials Science, Michigan State university, August 2003.
[4] Fluent User's Manual, Fluent Inc., Lebanon, New Hampshire, 2001.
[5] Hirt, C.W. & Nichols, B.D., Volume of Fluid (VOF) Method for Dynamics of Free Boundaries, J. Comput. Physics, 39:210-225, 1981.

Advances in Fluid Mechanics V, A. Mendes, M. Rahman & C. A. Brebbia (Editors)